Extraction of large valence-band energy offsets and comparison to theoretical values for strained-Si/strained-Ge type-II heterostructures on relaxed SiGe substrates

James T. Teherani,* Winston Chern, Dimitri A. Antoniadis, and Judy L. Hoyt
Massachusetts Institute of Technology (MIT), Cambridge, Massachusetts 02139, USA

Liliana Ruiz
University of Texas at Brownsville, Brownsville, Texas 78520, USA

Christian D. Poweleit and José Menéndez
Arizona State University, Tempe, Arizona 85287, USA

(Received 6 October 2011; revised manuscript received 22 February 2012; published 9 May 2012)

Metal-oxide-semiconductor capacitors were fabricated on type-II staggered gap strained-Si/strained-Ge heterostructures epitaxially grown on relaxed SiGe substrates of various Ge fractions. Quasistatic quantum-mechanical capacitance-voltage (CV) simulations were fit to experimental CV measurements to extract the band alignment of the strained layers. The valence-band offset of the strained-Si/strained-Ge heterostructure was found to be 770, 760, and 670 meV for 35, 42, and 52% Ge in the relaxed SiGe substrate, respectively. These values are approximately 100 meV larger than the usually recommended band offsets for modeling Si/Ge structures. It is shown that the larger valence-band offsets found here are consistent with an 800-meV average valence-band offset between Si and Ge, which also explains the type-II band alignment observed in strained-$Si_{1-x}Ge_x$ on unstrained-Si heterostructures.

DOI: 10.1103/PhysRevB.85.205308 PACS number(s): 73.20.−r, 71.70.Fk, 71.20.Mq

I. INTRODUCTION

The electronic band structure of tetrahedral semiconductors can be referred to a common energy scale from which the band offsets in the heterostructures can be derived,[1–5] including those involving alloys of these materials. In the case of Si and Ge, earlier *ab initio* calculations[5,6] indicated that in this common energy scale the "natural" valence-band offset between Si and Ge is about 500–600 meV, with the Ge valence band higher in energy. Starting from these values, the band lineups at specific heterojunctions can be predicted by performing appropriate strain corrections, which can be conveniently done by expressing the strain tensor as the sum of a hydrostatic contribution and a traceless shear component. People and Bean[7] proposed the following widely used expression, based on Van de Walle and Martin's 1985 theoretical work[8]:

$$\Delta E_v \text{ (in meV) for strained-Si/strained-Ge on (100) } Si_{1-xs}Ge_{xs} = 740 - 530xs, \quad (1)$$

where xs is the Ge fraction of the relaxed substrate and ΔE_v is the valence-band offset between strained-Si (s-Si) and strained-Ge (s-Ge) in millielectron volts. Rieger and Vogl introduced an expression for the *average* valence-band offset between s-Si and s-Ge[9]:

$$\Delta E_{v,av} \text{ (in meV) for strained-} Si_{1-x}Ge_x \text{ on (100) } Si_{1-xs}Ge_{xs} = (470 - 60xs)(x - xs), \quad (2)$$

where $\Delta E_{v,av}$ is the offset between the average valence-band energy of s-$Si_{1-x}Ge_x$ on a relaxed $Si_{1-xs}Ge_{xs}$ virtual substrate. The average energy of the top three valence bands ($E_{v,av}$) is unaffected by the shear component of the strain or by the spin-orbit interaction. The predictions from Eqs. (1) and (2) are quite similar. For the s-Ge/unstrained-Si interface, for example, Eq. (2) leads to $\Delta E_v = 700$ meV when valence-band splitting is taken into account, which is close to the value $\Delta E_v = 740$ meV from Eq. (1).

Despite their widespread use, the validity of Eqs. (1) and (2) for the prediction of the band lineups of Si-Ge heterostructures is not firmly established. This is remarkable in view of the intense scrutiny on this material system for over 40 years; however, the Si-Ge heterostructure is particularly difficult from the standpoint of band offset theory not just because of the large lattice mismatch but also because the conduction-band minima in Si and Ge are located at *different* points away from the Brillouin zone center. The calculation of the effect of strain on such states requires the use of several deformation potentials, which are not well known for *both* materials because most experimental probes provide values associated with the conduction-band minimum. A known (but not widely acknowledged) discrepancy between theory and experiment is the band alignment at s-$Si_{1-x}Ge_x$/unstrained-Si interfaces. Using Eqs. (1) and (2), or similar expressions, combined with experimental band gaps and reasonable choices for the strain deformation potentials, it can be shown that the band alignment is type I for s-$Si_{1-x}Ge_x$/unstrained-Si (valence-band maximum and conduction-band minimum both in the s-$Si_{1-x}Ge_x$ layer) for $x < 0.7$ (Refs. 6 and 10), whereas experimental results for s-$Si_{0.70}Ge_{0.30}$/unstrained-Si clearly show that the alignment is type II (lower conduction-band edge in Si).[11,12] Rieger and Vogl[9] *do* predict a type-II alignment for s-$Si_{0.70}Ge_{0.30}$/unstrained-Si, but they use theoretical hydrostatic deformation potentials for the Δ-minimum indirect band gap that differ from experimental values. Their theoretical deformation potential for Si is much larger and for Ge is of the opposite sign compared to experimental values.[13]

Interest in quantitatively understanding the type-II-staggered band alignment of tensile strained-Si on compressively strained-Ge grown on relaxed SiGe [shown in

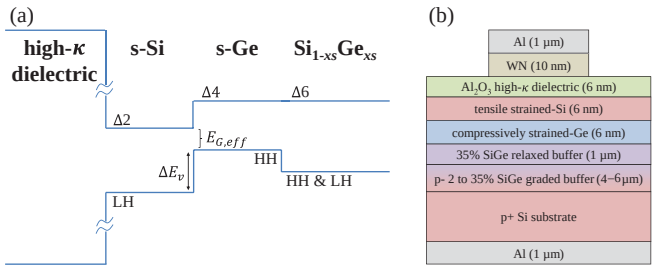

FIG. 1. (Color online) (a) Schematic energy band diagram illustrating the type-II band alignment between tensile strained-Si and compressively strained-Ge. The heavy-hole (HH) band is the topmost s-Ge valence band, and the $\Delta 2$ band is the bottom most s-Si conduction band. (b) MOS capacitor structure with a 35% SiGe relaxed buffer fabricated for valence-band offset extraction.

Fig. 1(a)] has been recently revived due to the relevance of this system in tunneling applications for which the current depends exponentially on the effective band gap between the Si conduction band and the Ge valence band.[14] In addition, the s-Si/s-Ge heterointerface is present in high-mobility-strained Ge channel *p*-metal-oxide-semiconductor field effect transistors (pMOSFETs), which are under study for future complementary MOS (CMOS) technology (e.g., Refs. 15–22). The valence-band offset determines the threshold voltage and gate-to-channel capacitance of such devices.

In view of the remaining discrepancies and the renewed interest in Si-Ge heterojunctions, we have performed new measurements of the valence-band offsets in this system using a quasistatic capacitance-voltage (QSCV) technique that is an extension of the method first described by Voinigescu *et al.*[23] We find that the valence-band offsets at the Si/Ge interface are much larger than predicted by Eqs. (1) and (2). Combining these results with a judicious choice of deformation-potential constants, we show that the newly determined band offsets can explain the long-standing puzzles in the heterostructure band alignment of the Si-Ge system.

II. FABRICATION OF HETEROSTRUCTURE MOS CAPACITORS

The final MOS capacitor structure for the s-Si/s-Ge on a relaxed 35% SiGe substrate is shown in Fig. 1(b). First, the initial SiGe layer (i.e., the graded buffer layer) was epitaxially grown at 900 °C on a (100)-oriented $p+$ Si substrate using an Applied Materials Epi Centura low-pressure chemical-vapor-deposition (LPCVD) system. The layer was *in situ* doped with boron at approximately 5×10^{16} cm^{-3}. To create a high-quality SiGe virtual substrate, the Ge alloy percentage of the initial SiGe layer was linearly graded from 2 to 35% over 4 μm of SiGe growth. Next, 1 μm of undoped relaxed 35% SiGe was grown on top of the graded buffer layer. Subsequently, approximately 6 nm of undoped compressively strained-Ge followed by 6 nm of undoped tensile strained-Si was grown on the surface of the SiGe virtual substrate. Similar growth procedures were used to also create s-Si/s-Ge heterostructures on 42 and 52% SiGe virtual substrates.

The epitaxial wafers underwent a modified RCA clean immediately before the high-κ dielectric deposition in an atomic layer deposition (ALD) system. A modified RCA clean was used to remove any contaminants while limiting removal of the thin s-Si layer, and it consisted of four key steps: (1) H_2SO_4:H_2O_2 (3:1) piranha clean, (2) diluted HF dip, (3) HCl:H_2O_2:H_2O (1:1:5) clean, and (4) diluted HF dip. The last HF dip removed any native SiO_2 that formed during the chemical cleaning. MOS capacitors were created by heating the sample to 250 °C in the ALD chamber and initially flowing 20% ozone *in situ* for 5 min. This was followed by the deposition of 6 nm of Al_2O_3 dielectric using trimethylaluminium (TMA) and water as precursors. These steps were followed by ALD of 10 nm of tungsten nitride (WN). Sputtered aluminum was used to create contacts at the top and bottom surfaces of the samples. The devices were patterned using typical photolithographic techniques to create MOS capacitors of various sizes. A final forming gas anneal was performed at 450 °C for 30 min, which dramatically lowered the density of interface traps at the Si/dielectric interface.

The Ge molar fraction in the relaxed buffer layer was measured by secondary ion mass spectrometry (SIMS) and micro-Raman spectroscopy using 514-nm excitation. The measured Ge content derived from each technique is listed in Table I. Whereas SIMS measures the Ge chemical concentration, Raman spectroscopy measures the shift in the vibrational frequencies of the atomic bonds of the crystal. Due to anharmonic and mass substitution effects, these frequencies are dependent on the strain state and Ge fraction of the SiGe alloy. The shift ($\Delta\omega$) of the alloy Si-Si Raman peak relative to the bulk Si Raman frequency is related to the Ge fraction by[24–26]

$$xs = -0.015 \cdot \Delta\omega. \tag{3}$$

This expression assumes that the SiGe layer is fully relaxed. Therefore, the excellent agreement between SIMS data and Raman-extracted Ge fraction indicates that the SiGe is nearly completely relaxed, as expected based upon the growth conditions. It should be noted that the Si and Ge layers are too thin for accurate measurements of strain using 514-nm excitation.

Ni Chleirigh performed an experimental analysis on the valence-band offset of the related s-Si/s-$Si_{1-x}Ge_x$ on relaxed $Si_{1-xs}Ge_{xs}$ heterostructure system;[27] however, her work only covered s-$Si_{1-x}Ge_x$ layers with up to 70% Ge. This paper expands that work by providing extraction of the band alignments for s-Si/s-Ge heterostructures on relaxed SiGe substrates of different Ge fractions, i.e., with different levels of biaxial strain in the heterostructure. Also, in contrast with the previous work, the present work employs a full-band quantum-mechanical simulator for the capacitance-voltage (CV) simulations.

III. PHYSICS OF THE CV EXTRACTION TECHNIQUE

A quasistatic CV (QSCV) measured from one of our samples is shown in Fig. 2. The band alignment extraction procedure originally developed by Kroemer *et al.*[28] for Schottky and *p-n* junction devices was expanded by Voinigescu *et al.*[23] to low-frequency CV measurements on high-quality MOS structures. Voinigescu found that the low-frequency CV curve of a Si/SiGe heterostructure MOS capacitor produces a distinctive plateau region (see region II of Fig. 2), which can be

TABLE I. Extracted and theoretical values for s-Si/s-Ge heterojunctions on different relaxed SiGe substrates. The experimental values were extracted by fitting quantum-mechanical simulations to experimental QSCV measurements. The theoretical values were calculated using an average valence-band offset of $\Delta E_{v,av} = 800$ meV between s-Si and s-Ge using the method described in Section VII: *Unified Theoretical Description of the Si-Ge section*.

	Measured Ge fraction of SiGe layer		Band alignments between s-Si/s-Ge layers					
			ΔE_v (meV)		$E_{G,\text{eff}}$ (meV)			
Name	SIMS	Raman	Exp.	Theory (this work)	Exp.	Theory (this work)	$E_{G,\text{Si}}$ (meV) Exp.	s-Si cap thickness (Å) Exp.
"35% SiGe"	35.5%	34.1%	770 ± 25	783	190 ± 50	137	960 ± 50	49 ± 2
"42% SiGe"	42.6%	41.3%	760 ± 25	755	185 ± 50	122	950 ± 50	45 ± 2
"52% SiGe"	52.7%	52.2%	670 ± 25	715	190 ± 50	101	860 ± 50	43 ± 2

used to extract the valence-band offset of the heterostructure. The valence-band offset extraction requires the material with a lower valence-band energy (in this case Si) to be at the surface of the heterostructure, thus producing a well for holes separated from the oxide/semiconductor surface.

The CV curve of the s-Si/s-Ge heterostructure MOS capacitor has four distinct regions illustrated in Figs. 2 and 3: hole accumulation in the Si and Ge layers (I), hole accumulation in the Ge layer (II), depletion of holes (III), and electron inversion in the Si layer (IV). The maximum capacitance of regions I and IV allow fitting of the dielectric thickness to an equivalent oxide (SiO_2) thickness (EOT), while region II, which we call the plateau region, allows for determination of the s-Si thickness and valence-band offset at the s-Si/s-Ge interface. The narrow width of region III is indicative of the small effective band gap ($E_{G,\text{eff}} = E_{c,\text{Si}} - E_{v,\text{Ge}}$) of the s-Si/s-Ge heterostructure.

In a *p*-type s-Si/s-Ge heterostructure MOS capacitor, represented in Figs. 2 and 3, as the gate voltage is swept from positive to negative, holes are first accumulated in the buried s-Ge quantum well (region II) and then eventually at the s-Si/dielectric interface as a more negative gate bias is applied (region I). The plateau width in region II is directly related to the valence-band offset. As the valence-band offset increases, increased negative gate voltage is required to bend the Si valence bands toward the Fermi level in order to accumulate the Si layer with holes, and this causes an increase in the plateau width (region II) of the CV curve. The plateau width of the simulated CV data is fit to the experimental data by varying the s-Si/s-Ge valence-band offset of the simulation.

The capacitance of the plateau region (region II) is approximately given by the series combination of the oxide and Si layer capacitances because the unpopulated Si layer acts as a dielectric. During the transition from region II to region I, as the gate bias is swept to more negative voltages, holes begin to populate the Si layer as the Si valence bands bend toward the Fermi level. The Si layer no longer acts as a dielectric, and the capacitance increases toward the oxide capacitance due to the decrease of the effective dielectric thickness.

Region III of the CV curve provides information about effective band gap, $E_{G,\text{eff}}$, at the s-Si/s-Ge heterojunction,

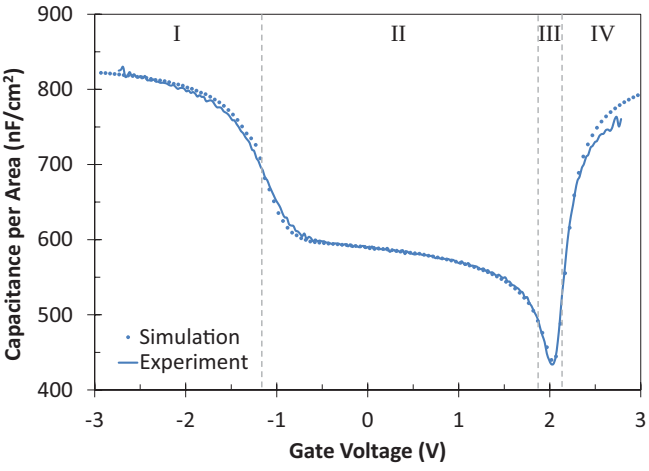

FIG. 2. (Color online) Experimental and simulated QSCV curves for s-Si/s-Ge on a relaxed 35% SiGe substrate. The following parameters were used to produce the simulated CV curve: 38 Å EOT, 49 Å s-Si cap thickness, $\Delta E_v = 770$ meV, and $E_{G,\text{eff}} = 190$ meV. The CV analysis does not provide significant sensitivity to other parameters. Voltage regions of distinct carrier distributions are identified by Roman numerals and described in the text and shown schematically in Fig. 3.

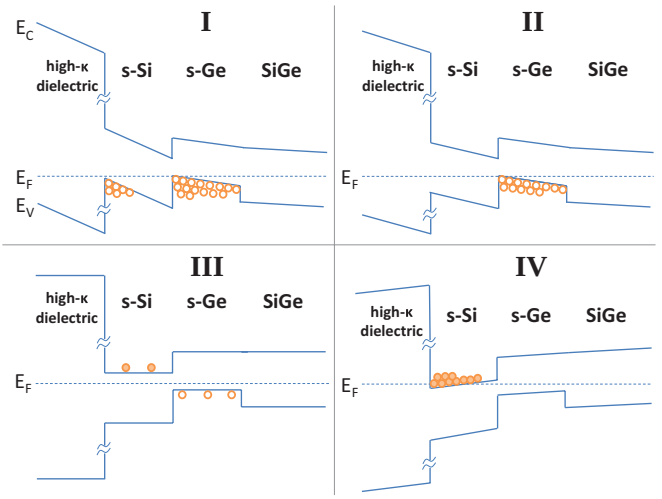

FIG. 3. (Color online) Depiction of the heterostructure band diagrams and carrier populations (not drawn to scale) under the different regimes labeled in Fig. 2.

which is given by

$$E_{G,\text{eff}} = E_{c,\text{Si}} - E_{v,\text{Ge}}, \tag{4a}$$

$$= E_{G,\text{Si}} - \Delta E_v, \tag{4b}$$

where $E_{c,\text{Si}}$ is the conduction-band-edge energy of s-Si, $E_{v,\text{Ge}}$ is the valence-band-edge energy of s-Ge, $E_{G,\text{Si}}$ is the band gap of s-Si, and ΔE_v is the valence-band offset at the s-Si/s-Ge heterojunction. For a given s-Si band gap, an increase in ΔE_v suggests a decrease in $E_{G,\text{eff}}$ by the same amount.

Due to the small effective band gap of the heterostructure, electrons begin to collect in the Si conduction band before holes are fully depleted from the structure. Thus, the width of region III is very narrow, and the capacitance of region III does not decrease to the low values typically measured in Si homostructure MOS capacitors in depletion. $E_{G,\text{eff}}$ is directly related to the width and capacitance of region III, and $E_{G,\text{Si}}$ (the sum of ΔE_v and $E_{G,\text{eff}}$) is directly related to the total width of regions II and III. The band alignment of s-Si/s-Ge can be extracted by varying ΔE_v and $E_{G,\text{eff}}$ of the simulation structure until a good fit is found between simulated and experimental CV. Because ΔE_v and $E_{G,\text{eff}}$ affect different regions of the CV curve, their values can be extracted independently.

IV. MEASUREMENT AND EXPERIMENTAL DETAILS

The CV curves were measured using a quasistatic method. For this technique, an Agilent 4156C Parameter Analyzer was used to apply a dc bias across the device. The parameter analyzer steps the voltage and integrates the current to determine the change in charge, ΔQ, that occurred over the voltage step, ΔV. The equipment also applies some basic algorithms to mitigate the effect of integrating oxide leakage current. A detailed description of the technique is given in Ref. 29. The QSCV method has the advantage that it emulates the quasistatic simulation technique and is able to probe the inversion regime of the CV curve. The inversion regime is difficult to measure with low-frequency CV due to the long carrier lifetimes attributed to the high quality of the epitaxial layers and $1/f$ noise that becomes substantial at frequencies less than 1 kHz.

The measurements shown in this paper were made using the QSCV technique on unpackaged samples in a dark, electromagnetically shielded probe station at room temperature. Voltage steps of 24 mV were used, with 500 ms of quasistatic integration time and 100 ms of leakage current integration time (which the 4156 algorithm uses to remove the effects of gate leakage). Devices were screened to ensure low dc gate leakage and high-quality dielectric. The dc leakage current through the dielectric of the MOS capacitors was measured to be less than 1 nA/cm^2 in the voltage range from -2 to 2.75 V. There was good agreement between low-frequency and QSCV measurements for ac frequencies less than 500 Hz. Alternating-current CV measurements at frequencies higher than 500 Hz showed a decrease in the inversion capacitance due to long carrier lifetimes in the high-quality material. The observed hysteresis between positive- and negative-directed voltage sweeps was less than 20 mV, indicating a high-quality dielectric.

A requirement for obtaining clean QSCV data reflecting only the semiconductor band structure is that the dielectric/semiconductor interface be of high quality. In our laboratory, significant work has been conducted on the deposition of high quality Al_2O_3 on Si and s-Si/s-Ge heterostructures with minimal density of interface traps (D_{it}) and mobile oxide charge that causes hysteresis.[30–33] In the present work, the D_{it} of a Si control wafer with the same Al_2O_3 procedure as used for the heterostructure wafers was measured to be $\sim 10^{11}$ $\text{cm}^{-2}\text{eV}^{-1}$ at midgap by using the conductance method.[34,35] Simulations incorporating D_{it} (not shown in this paper) suggest that at values determined from the Si control wafer, there is minimal impact on the valence-band extraction method. Though the D_{it} of the Si control wafer may be considered a lower bound for the expected D_{it} of the heterostructure wafers, other features of the measured CV curves of the heterostructure devices also suggest a low D_{it}. After accounting for series resistance, a capacitance offset, which would suggest the presence of D_{it}, does not appear between the high- and low-frequency CV curves when transitioning from accumulation to depletion. Furthermore, a large D_{it} would stretch out the CV curve, yielding a larger value for the valence-band offset *and* for the s-Si band gap. However, the extracted s-Si band gap, shown in Fig. 7(a), is slightly lower than expected based on previous experiments and theory, which signifies a small D_{it} that has minimal impact on the extraction technique. Moreover, the slope of the experimental CV curve at the point where holes begin to accumulate in the s-Si layer (transitioning from region II to region I in Fig. 2) would also be stretched out by a large D_{it}. But the simulation without D_{it} matches the experimental data well as shown in Fig. 2, which is consistent with a small D_{it}.

Although a large hole barrier (i.e., the valence-band offset) exists between the s-Si and s-Ge (shown in region I of Fig. 3), limiting the rate at which holes can populate the s-Si layer, the slow voltage sweep rate of the quasistatic measurement method allows enough time for the carriers to respond so that quasiequilibrium can be reached between each voltage step. Ultimately, the path that the holes take (whether through thermionic emission or tunneling through the large valence-band barrier) to populate either of the quantum wells does not impact the QSCV measurement. What *is* important is that the carriers reach quasiequilibrium between each voltage step so that the change in charge in each quantum well is representative of the quasiequilibrium simulations.

V. RESULTS AND SIMULATIONS

The simulated QSCV capacitance curve was calculated by taking the numerical derivative of the change of integrated charge density in the semiconductor layers divided by the voltage step ($C = dQ/dV$). An advanced simulation tool that accounts for quantum-mechanical effects and band splitting due to strain is necessary to properly model the charge density at different voltages. Whereas Ni Chleirigh[36] used a single-band simulator with a density gradient model for quantum corrections and a modified valence-band density of states N_v to account for strain,[37] this work uses *nextnano3* (Refs. 38 and 39), a full-band quantum-mechanical simulator. With *nextnano3*, we model multiple valence bands with a

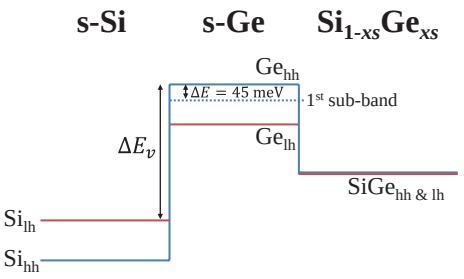

FIG. 4. (Color online) Valence-band diagram of the s-Si/s-Ge/relaxed SiGe heterostructure. The heavy hole (hh) and light hole (lh) valence bands in s-Si and s-Ge split due to tensile and compressive strain, respectively. The valence-band offset quoted in this paper is the difference between the top valence-band edges of s-Ge and s-Si. The simulation models quantization effects, but only the band-edge difference is quoted in order to provide information about the band lineup that is independent of the quantum well thicknesses.

6×6 $k \cdot p$ method that captures the nonparabolic valence-band structure with strain. Additionally, the Schrödinger-Poisson equation is solved self-consistently to determine the charge density that is then used to calculate the capacitance.

A comparison of the measured and fitted simulation QSCV is shown in Fig. 2 for s-Si/s-Ge on a relaxed 35% SiGe substrate. The extracted valence-band offset and effective band gap for the sample are $\Delta E_v = 770 \pm 25$ meV and $E_{G,\text{eff}} = 190 \pm 50$ meV, respectively. The quoted uncertainty reflects the range of these parameter values that yields a qualitatively good fit between simulation and experimental data. The extracted EOT and s-Si cap thicknesses are 38 ± 2 Å and 49 ± 2 Å, respectively, in agreement with values expected from the fabrication processes used.

In this paper we use the standard definition of valence-band offset: the energy difference between the valence-band maxima at both sides of a heterojunction between two semi-infinite materials. In the case of a Si/Ge heterostructure strained to SiGe, this definition corresponds to the difference between the s-Ge heavy-hole valence-band edge and the s-Si light-hole valence-band edge, as shown in Fig. 4. The simulation includes the effects of quantization, but the valence-band offset is quoted as the difference in the band edges. While the figure uses the terms *heavy hole* (hh) and *light hole* (lh) to identify the split valence bands, it should be noted that even at $k = 0$, the strain Hamiltonian mixes the light and split-off band.[40]

In general, good agreement is obtained between experimental and simulated CV curves, with high sensitivity to the following parameters: EOT (i.e., equivalent [SiO_2] oxide thickness of the dielectric), Si thickness, valence-band offset, and effective band gap. Other parameters, such as the doping concentration, have a weaker impact on the simulation results. Additionally, the EOT, Si thickness, and valence-band offset can be extracted independently from other simulation variables. The maximum capacitance determines the EOT. As shown in Fig. 5, the Si thickness affects the plateau capacitance, which is the series combination of the oxide and Si capacitances. The Si layer acts as a dielectric in the plateau region of the CV curve because of the low carrier density in Si. Increasing the Si thickness effectively increases the dielectric thickness and results in a lower capacitance in

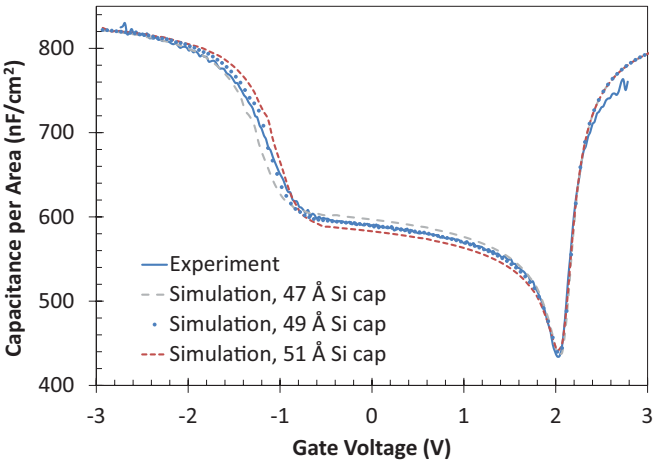

FIG. 5. (Color online) Simulated QSCV for different s-Si cap thicknesses. The simulated CV displays a high sensitivity to small changes in the s-Si cap thickness, which allows the physical thickness to be extracted with low uncertainty (±2 Å).

the plateau region of the CV curve, and the high sensitivity to small changes in the s-Si thickness enables low uncertainty (±2 Å) in its extraction. As discussed earlier, the s-Si/s-Ge valence-band offset modifies the plateau width, as shown in Fig. 6. The effective band gap, $E_{G,\text{eff}}$, is not as easily extracted because changes in the effective band gap and doping in the SiGe both produce similar effects on the simulation CV curve in region III, and these parameters are not easily decoupled. For this reason, the uncertainty of the extracted effective band gap is larger than the quoted uncertainty of the valence-band offset.

The sensitivity of the extraction method to changes in ΔE_v is illustrated in Fig. 6 for a 35% SiGe substrate. For these structures, a small change in the valence-band offset produces about a four times larger change in the width of the plateau region (e.g., a 50-meV increase in ΔE_v produces a ~200-mV enlargement of the plateau width). The extracted values for the

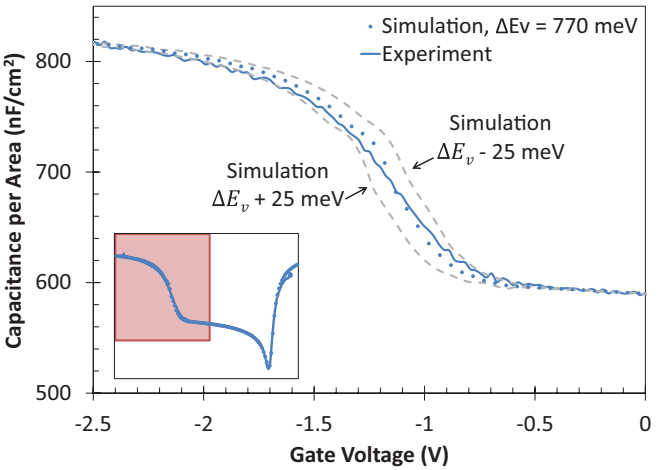

FIG. 6. (Color online) Measured and simulated CV curves illustrating the high sensitivity of the simulation to ΔE_v. A 25-meV change in ΔE_v produces about a 90-mV change in the plateau width. A change in ΔE_v only impacts the portion of the CV curve shown here.

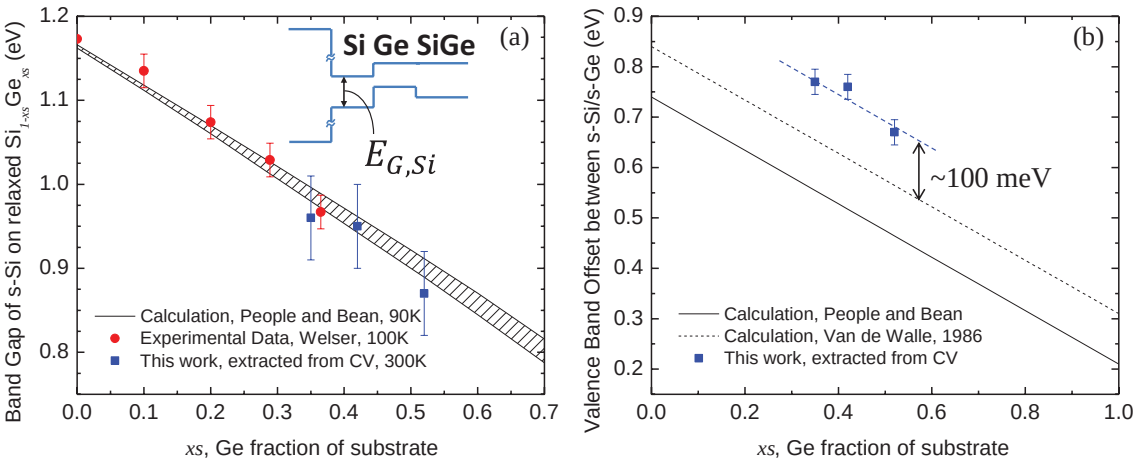

FIG. 7. (Color online) (a) Calculations by People and Bean[7] of the band gap of s-Si for different Ge fractions of the relaxed $Si_{1-x}Ge_x$ substrate compared to values extracted from CV analysis in this work. The experimental data from Welser[24] is also included for comparison. (b) Valence-band offset, ΔE_v, as a function of Ge fraction in the substrate. People and Bean[7] calculate a linear relation from theoretical work by Van de Walle and Martin in 1985 (Ref. 8). The dotted line is a linear relationship derived from updated calculations in Van de Walle and Martin's 1986 paper.[6] The valence-band offsets extracted in this work are about 100 meV larger than the linear relationship derived from theoretical values of Ref. 6.

valence-band offset, effective band gap, and silicon band gap are shown in Table I.

VI. DISCUSSION

Figure 7(a) compares the theoretical values of the s-Si band gap from Ref. 7 with values extracted in this work as a function of substrate Ge fraction (xs). Also plotted are Welser's experimental data[24] extracted using a MOS CV technique for s-Si grown directly on relaxed SiGe. The data show that the band gap of s-Si decreases as biaxial strain in the silicon is increased (increasing xs), and the values are in reasonable agreement with People and Bean's calculated values. However, Fig. 7(b) shows that the extracted valence-band offset between s-Si/s-Ge is about 200 meV greater than Eq. (1) and 100 meV greater than a linear relationship derived from Van de Walle and Martin's updated 1986 theoretical values (Ref. 6).

Because ΔE_v is roughly 100 meV larger than reported calculated values, we find $E_{G,\text{eff}}$ to be significantly smaller than previously expected [$E_{G,\text{eff}}$∼190 meV versus 300–400 meV based on Eqs. (1) and (2)].

Interestingly, $E_{G,\text{eff}}$ remains relatively constant as a function of the substrate Ge fraction, xs, as shown in Table I. As xs increases, biaxial tensile strain in the s-Si increases and biaxial compressive strain in the s-Ge decreases. Increasing strain in s-Si causes the silicon valence and conduction bands to move toward one another, whereas decreasing strain in s-Ge causes the germanium valence and conduction bands to move apart. The net result is that both the s-Si conduction band and s-Ge valence band move lower in energy with increasing xs so that $E_{G,\text{eff}}$ remains relatively constant. The same effect causes ΔE_v to decrease with increasing xs. The movement of the bands with strain is shown schematically in Fig. 8.

The valence-band offset extracted in this work is compared to previous experimental work on s-Si/s-$Si_{1-x}Ge_x$ heterojunction grown on relaxed $Si_{1-xs}Ge_{xs}$ in Fig. 9, and the value extracted in this work for s-Si/s-Ge on ∼40% SiGe substrate is in good agreement with the extrapolated value from Ni Chleirigh's data.

VII. UNIFIED THEORETICAL DESCRIPTION OF THE Si-Ge SYSTEM

The calculation of band lineups based on common reference levels is described in detail by Van de Walle.[4] The starting point is the average energy $E_{v,av}$ of the top three valence bands of each bulk, unstrained semiconductor. For elemental and binary compounds, these averages can be predicted theoretically on a common energy scale. The corresponding energies for alloys are interpolated following Ref. 41. The average energy $E_{v,av}$ is a convenient reference because it is unaffected by either the shear component of the strain or the spin-orbit interaction. When a strained heterojunction is formed, only the hydrostatic component of the strain affects the $E_{v,av}$ energies. The corresponding shifts can be calculated using the absolute valence-band deformation potentials, a_v, for each material. The shear strain and the spin-orbit interaction split the electronic bands in ways that can be computed using standard deformation-potential theory. For the case of unstrained Si/Ge, $\Delta E_{v,av}$ between Si and Ge was calculated to be between 500 and 700 meV.[5,6] Using the deformation potentials in Table II, which are justified in the Appendix, we adjusted the value of $\Delta E_{v,av}$ to reproduce the 40-meV type-II band

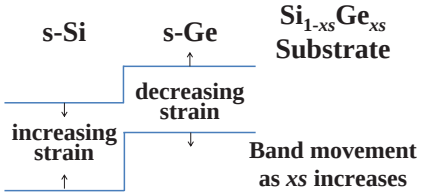

FIG. 8. (Color online) Illustration of the changes in the band edges with increased Ge fraction in the substrate (xs).

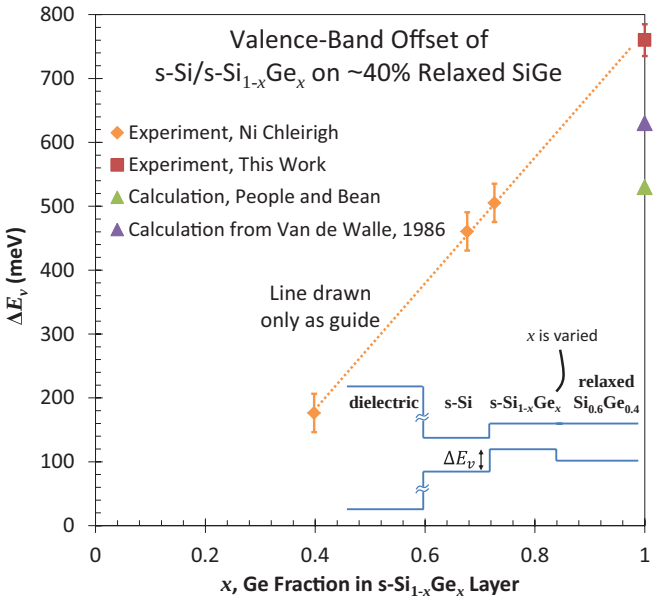

FIG. 9. (Color online) Valence-band offset for s-Si/s-$Si_{1-x}Ge_x$ grown on a relaxed SiGe substrate with ~40% Ge, as a function of Ge fraction in the s-$Si_{1-x}Ge_x$ layer. The inset shows a depiction of the heterostructure band diagram highlighting the valence-band offset. Ni Chleirigh[36] extracted the valence-band offset using a CV technique similar to this work. Both calculations shown in the plot are linear relations derived from theory by Van de Walle and Martin. People and Bean[7] calculate a linear relation from Van de Walle and Martin's 1985 paper,[8] while the purple (dark gray) data point is calculated using updated values from Van de Walle and Martin's 1986 paper.[6]

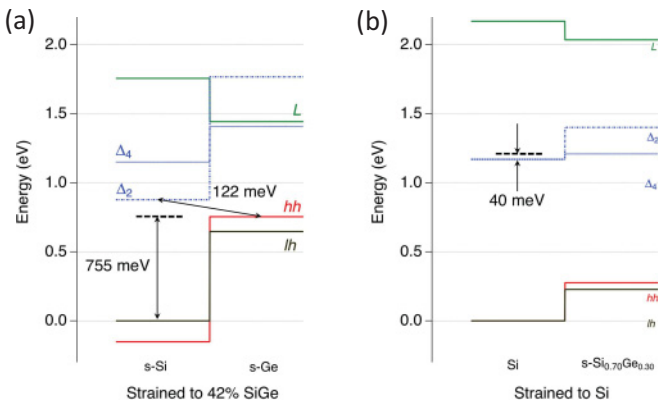

FIG. 10. (Color online) Calculated band lineups of the (a) s-Si/s-Ge heterostructure pseudomorphic to 42% SiGe and (b) s-$Si_{0.70}Ge_{0.30}$/Si heterostructure pseudomorphic to Si using standard deformation potential theory. The calculations assume that the average valence-band offset between Si and Ge is $\Delta E_{v,av} = 800$ meV.

offset at the $Si_{0.70}Ge_{0.30}$/Si, as observed by Thewalt *et al.*[11] We obtain an exact fit using $\Delta E_{v,av} = 800$ meV. Using this value without any other adjustments, we then calculate the band offsets and effective band gaps in our three samples using standard deformation-potential theory. These are shown as the theoretical entries in Table I.

Representative band lineups calculated with standard deformation-potential theory are shown in Fig. 10. We find a remarkable agreement of the theoretical predictions with the experimental data, particularly when one takes into account that we are assuming linear elasticity and deformation-potential theory in the presence of very large biaxial strains of up to 2% in Si and -2.7% in Ge. The extracted and theoretical valence-band offsets are well within experimental error for two samples and marginally outside experimental error for the sample with the largest strain on the Si layer, whereas the effective band gaps are just below the lower end of the experimental error bar. These effective band gaps, as mentioned above, are more difficult to extract from the data, and their theoretical values are also more sensitive to the exact values of the deformation potentials. Had we computed the sample shown in Fig. 10 using $\Delta E_{v,av} = 600$ meV, a value considered until now to be consistent with experiment, we would have obtained $\Delta E_v = 550$ meV and $E_{G,\text{eff}} = 320$ meV, in strong disagreement with our experimental results. It is also worth noting that the calculations reproduce the weaker dependence of the effective band gap on the substrate composition.

Our results imply a band offset $\Delta E_v = 910$ meV for the s-Ge/Si interface, much larger than expected from Eq. (1). It is instructive to compare our results with core-level spectroscopy measurements of the band offsets. In these experiments, the band edges are measured relative to core levels. The band offsets follow immediately from the data if the core levels are independent of the volume (i.e., if their absolute hydrostatic deformation potential is zero). This, however, is not necessarily the case. Schwartz and coworkers[42] find $\Delta E_v = 740 \pm 130$ meV for s-Ge on Si, in agreement with Eq. (1), using theoretical Si $2p$ and Ge $3d$ deformation potentials, which are not known independently, so that the accuracy of their result is difficult to assess. Morar *et al.*[43] introduced a very elegant transmission electron energy loss method that yields $\Delta E_{v,av}$ between Ge and Si directly from measurements of the Si $2p$ conduction-band absorption edge in relaxed $Si_{1-x}Ge_x$ alloys. They find $\Delta E_{v,av} = 690$ meV. However, in their estimate of the correction to the assumption of a constant Si $2p$ level, they compute a volume deformation potential of 2 eV for the $2p$ level. More detailed calculations by Franceschetti *et al.*,[44] give -0.1 eV for the same deformation potential. If we

TABLE II. Selected deformation potentials for Si and Ge in eV. The notation is as in Ref. 4, and the values are explained in the Appendix. For alloys, the deformation potentials are linearly interpolated.

	Valence-band absolute deformation potential, a_v	Valence-band shear deformation potential, b	Hydrostatic deformation potential, $(\Xi_d + \frac{1}{3}\Xi_u - a_v)^\Delta$	Conduction-band shear deformation potential, Ξ_u^Δ
Si	2.24	-1.73	1.47	8.70
Ge	2.10	-1.88	1.80	8.95

recompute Morar's results using the Franceschetti deformation potential, we find that their measurements imply $\Delta E_{v,av} =$ 770 meV, in much better agreement with our results. Moreover, the most recent *ab initio* calculations of band offsets[45] yield $\Delta E_{v,av} = 750$ meV for the Si-Ge system, which is also closer to our results than previous *ab initio* predictions.

VIII. SUMMARY

The valence-band offsets for s-Si/s-Ge heterojunctions pseudomorphic to various relaxed SiGe substrates were extracted by fitting full-band quantum-mechanical simulations to experimental QSCV measurements on MOS capacitors. Good agreement was found between simulated and measured CV curves with high sensitivity to the valence-band offset of the s-Si/s-Ge heterostructure. Values of $\Delta E_v = 770$, 760, and 670 meV were obtained for 35, 42, and 52% Ge fraction SiGe substrates respectively. The effective band gap was found to be about 190 meV, irrespective of the substrate Ge fraction.

The large valence-band offsets measured in this paper as well as the observation of type-II alignment in s-$Si_{1-x}Ge_x$/Si heterojunctions by Thewalt *et al.* can be simultaneously explained by assuming an average valence-band offset, $\Delta E_{v,av} = 800$ meV between Si and Ge. This value is much larger than usually assumed in simulations of the of the Si-Ge system.

ACKNOWLEDGMENTS

This work was completed at the MIT Microsystems Technology Laboratories with support from DARPA under Contract No. FA8650-08-C-7835, the NSF Center for Energy Efficient Electronics Science under NSF Contract No. ECCS-0939514, and an NDSEG Department of Defense Fellowship. Author J. M. is supported by the NSF under Grant No. DMR-0907600.

APPENDIX

As indicated in the introduction, the use of several deformation potentials with different degrees of uncertainty is unavoidable when analyzing Si-Ge heterostructures. The most important parameters that affect our calculations are given in Table II. It should be stressed, however, that our main conclusion, namely that the Si-Ge valence-band offset is larger than hitherto assumed, is not significantly affected by the particular choice of deformation potentials. For example, using the *theoretical* deformation potentials from Van de Walle[4] and following the same procedure used above, we find that the offset that reproduces Thewalt's photoluminescence results[11] is $\Delta E_{v,av} = 720$ meV, which is also very large. When applied to our s-Si/s-Ge heterostructure, this model gives somewhat better effective band gaps and somewhat worse band offsets. Nevertheless, we believe that the deformation potentials presented in Table II represent a better choice, and we briefly summarize how they were obtained.

For the absolute deformation potentials, we start with the experimental pressure dependence of the direct band gap E_0 in Ge, as measured by Goñi *et al.*[46] They find that the resulting volume dependence of the band-gap energy is not exactly linear, so we fit a linear expression over the range of volume changes (~0 to 2.5%) likely to be found in epitaxially strained systems. We obtain a band-gap volume deformation potential, $a_c - a_v = -9.47$ eV. Here we express the band-gap deformation potential in terms of the absolute deformation potentials for the conduction and valence bands at the Γ-point of the Brillouin zone, a_c and a_v. These have been calculated theoretically by several groups. We use values from Li *et al.*[47] who obtain $a_c = -7.83$ eV and $a_v = 2.23$ eV, in good agreement with Ge band-gap data ($a_c - a_v = -10.06$ eV). We correct for the residual small deviation by multiplying the theoretical values by a factor $9.47/10.06 = 0.94$ to match the band-gap data exactly. This gives the value listed in Table II, $a_v = 2.10$. For Si, there are no pressure dependence studies of E_0. Therefore, we take the value of a_v from Ref. 44 and "renormalize" with the same factor used for Ge. The resulting absolute deformation potentials in Table II are in excellent agreement with the values needed to fit the hole mobilities in Si and Ge.[48]

From the pressure dependence of the fundamental band gap of Si,[49] we obtain the hydrostatic deformation potential $(\Xi_d + \frac{1}{3}\Xi_u - a_v)^{\Delta} = 1.47$ eV for Si. The pressure dependence of the indirect gap associated with the Δ-valley in Ge has been measured by Ahmad and Adams,[13] and from their measurements, we obtain $(\Xi_d + \frac{1}{3}\Xi_u - a_v)^{\Delta} = 1.80$ eV for Ge.

The shear deformation potentials that give the splitting of bands due to the traceless component of the strain tensor are traditionally measured in uniaxial stress experiments, which potentially suffer from stress calibration issues, as suggested by the fact that Raman phonon Grüneisen parameters obtained from such experiments do not agree very well with direct hydrostatic pressure measurements in diamond anvil cells.[50–53] In the case of the valence-band shear deformation potential, Liu *et al.*[54] recently determined $b = 1.88$ eV for Ge using strained-layer Ge films in which the strain was measured with high-resolution x-ray diffraction. It is interesting to point out that the hydrostatic deformation potential obtained by these authors agrees exactly with the value obtained from Goñi *et al.*[46] when the data from the latter is fit over the same volume change range. We use Liu's value for Ge, and for Si, we take the

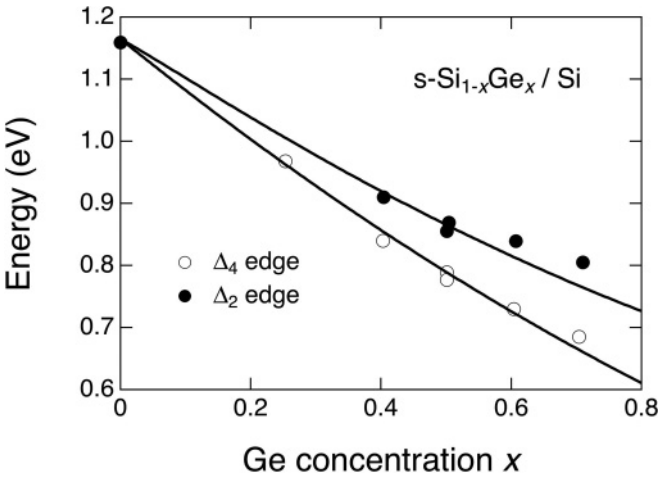

FIG. 11. Experimental Δ-like absorption edges of strained $Si_{1-x}Ge_x$ alloys on relaxed Si substrates from Lang *et al.* (circles; Ref. 57), and our calculation of these edges (lines) using the experimental compositional dependence of the band gap in relaxed $Si_{1-x}Ge_x$ alloys from Ref. 58 and the deformation potentials in Table II.

Ge value for b and multiply times the theoretically predicted ratio of this quantity for Si and Ge.[4] Finally, for the shear deformation potential for Si associated with the Δ-minimum of the conduction band, we use the value measured by Laude *et al.*,[55] $\Xi_u = 8.7$ eV. There are no equivalent measurements for Ge, but most theoretical calculations give values slightly larger than similar calculations for Si that are in good agreement with the experimental data. Accordingly, we use $\Xi_u = 8.95$ eV for Ge, which follows from multiplying the Si value from Laude[55] times the theoretical ratio for Ξ_u for Ge and Si.[4] Assuming linear interpolation of the deformation potentials for $Si_{1-x}Ge_x$, the predicted dependence of the split indirect band gaps in $Si_{1-x}Ge_x$ alloys pseudomorphic to Si substrates is compared with experimental data in Fig. 11.

As a final comment, we point out that in 1991, Li and coworkers[56] introduced a capacitance method from which the shear deformation potential Ξ_u can be obtained quite straightforwardly from samples under uniaxial stress. They find $\Xi_u =$ 11.3 eV for Si, significantly larger than the value above from Laude,[55] and they present a very thorough discussion of the errors associated with different experiments. We suspect that the discrepancies between different authors are due in part to differences in the calibration of their stress apparatuses, as suggested above. In the case of Laude, the hydrostatic deformation potentials deduced from their experiment agree very well with the direct hydrostatic pressure measurements in Ref. 48, suggesting small stress calibration errors. No corresponding hydrostatic data comparison is presented by Li. Moreover, if we use Li's value for Ξ_u, the agreement between theory and experiment in Fig. 11 worsens, so we prefer to use Laude's value until Li's shear-deformation-potential value is confirmed by new experiments.

*teherani@mit.edu

[1] F. Flores and C. Tejedor, J. Phys. C **12**, 731 (1979).
[2] J. Tersoff, Phys. Rev. B **30**, 4874 (1984).
[3] M. Cardona and N. E. Christensen, Phys. Rev. B **35**, 6182 (1987).
[4] C. G. Van de Walle, Phys. Rev. B **39**, 1871 (1989).
[5] L. Colombo, R. Resta, and S. Baroni, Phys. Rev. B **44**, 5572 (1991).
[6] C. G. Van de Walle and R. M. Martin, Phys. Rev. B **34**, 5621 (1986).
[7] R. People and J. C. Bean, Appl. Phys. Lett. **48**, 538 (1986).
[8] C. G. Van de Walle and R. M. Martin, J. Vac. Sci. Technol. B **3**, 1256 (1985).
[9] M. M. Rieger and P. Vogl, Phys. Rev. B **48**, 14276 (1993).
[10] G. Abstreiter, *Light Emission in Silicon: From Physics to Devices* (Academic Press, San Diego, 1998), p. 37.
[11] M. L. W. Thewalt, D. A. Harrison, C. F. Reinhart, J. A. Wolk, and H. Lafontaine, Phys. Rev. Lett. **79**, 269 (1997).
[12] C. Penn, F. Schäffler, G. Bauer, and S. Glutsch, Phys. Rev. B **59**, 13314 (1999).
[13] C. N. Ahmad and A. R. Adams, Phys. Rev. B **34**, 2319 (1986).
[14] O. M. Nayfeh, C. Ni Chleirigh, J. Hennessy, L. Gomez, J. L. Hoyt, and D. A. Antoniadis, IEEE Electron Device Lett. **29**, 1074 (2008).
[15] A. Ritenour, S. Yu, M. L. Lee, N. Lu, W. Bai, A. Pitera, E. A. Fitzgerald, D. L. Kwong, and D. A. Antoniadis, *Electron Devices Meeting, 2003. IEDM '03 Technical Digest. IEEE International* (IEEE, Washington, DC, 2003), pp. 18.2.1–18.2.4.
[16] R. Pillarisetty, B. Chu-Kung, S. Corcoran, G. Dewey, J. Kavalieros, H. Kennel, R. Kotlyar, V. Le, D. Lionberger, M. Metz, and others, *Electron Devices Meeting (IEDM), 2010. IEEE International* (IEEE, San Francisco, CA, 2010), pp. 6.7.1–6.7.4.
[17] M. L. Lee and E. A. Fitzgerald, *Electron Devices Meeting, 2003. IEDM '03 Technical Digest. IEEE International* (IEEE, Washington, DC, 2003), p. 18-1.
[18] H. Shang, J. O. Chu, S. Bedell, E. P. Gusev, P. Jamison, Y. Zhang, J. A. Ott, M. Copel, D. Sadana, K. W. Guarini, and others, *Electron Devices Meeting, 2004. IEDM Technical Digest. IEEE International* (IEEE, San Francisco, CA, 2004), pp. 157–160.
[19] S. W. Bedell, A. Majumdar, J. A. Ott, J. Arnold, K. Fogel, S. J. Koester, and D. K. Sadana, IEEE Electron Device Lett. **29**, 811 (2008).
[20] T. Krishnamohan, Z. Krivokapic, K. Uchida, Y. Nishi, and K. C. Saraswat, IEEE Trans. Electron Devices **53**, 990 (2006).
[21] G. Nicholas, T. Grasby, D. Fulgoni, C. Beer, J. Parsons, M. Meuris, and M. Heyns, IEEE Electron Device Lett. **28**, 825 (2007).
[22] O. Weber, Y. Bogumilowicz, T. Ernst, J. M. Hartmann, F. Ducroquet, F. Andrieu, C. Dupre, L. Clavelier, C. Le Royer, N. Cherkashin, and others, *Electron Devices Meeting, 2005. IEDM Technical Digest. IEEE International* (IEEE, Washington, DC, 2005), pp. 137–140.
[23] S. P. Voinigescu, K. Iniewski, R. Lisak, C. A. T. Salama, J.-P. Noél, and D. C. Houghton, Solid-State Electron. **37**, 1491 (1994).
[24] J. J. Welser, Ph.D thesis, Stanford University, 1995.
[25] B. Dietrich, E. Bugiel, J. Klatt, G. Lippert, T. Morgenstern, H. J. Osten, and P. Zaumseil, J. Appl. Phys. **74**, 3177 (1993).
[26] H. K. Shin, D. J. Lockwood, and J.-M. Baribeau, Solid State Commun. **114**, 505 (2000).
[27] Ni Chleirigh, Ph.D thesis, MIT, 2007.
[28] H. Kroemer, W.-Y. Chien, J. S. Harris, and D. D. Edwall, Appl. Phys. Lett. **36**, 295 (1980).
[29] Agilent Application Notes: Evaluation of Gate Oxides Using a Voltage Step Quasi-Static CV Method.
[30] P. Hashemi, J. T. Teherani, and J. L. Hoyt, *Electron Devices Meeting (IEDM), 2010 IEEE International* (San Francisco, CA, 2010), pp. 34.5.1–34.5.4.
[31] P. Hashemi, Ph.D thesis, MIT, 2010.
[32] P. Hashemi and J. L. Hoyt, IEEE Electron Device Lett. **33**, 173 (2012).
[33] J. Hennessy, Ph.D thesis, MIT, 2010.
[34] D. K. Schroder, *Semiconductor Material and Device Characterization*, 3rd ed. (Wiley-IEEE Press, Hoboken, NJ, 2006).
[35] E. Nicollian and A. Goetzberger, Bell Syst. Tech. J. **46**, 1055 (1967).
[36] C. Ni Chleirigh, C. Jungemann, J. Jung, O. O. Olubuyide, and J. L. Hoyt, *Proceedings of the Electrochemical Society: SiGe: Materials, Processing and Devices* (Honolulu, HI, 2005), pp. 99–10.
[37] ISE Dessis simulator—no longer available and now part of Synopsys Sentaurus Device.
[38] S. Birner, S. Hackenbuchner, M. Sabathil, G. Zandler, J. A. Majewski, T. Andlauer, T. Zibold, R. Morschl, A. Trellakis, and P. Vogl, Acta Phys. Pol. A **110**, 111 (2006).
[39] S. Birner, T. Zibold, T. Andlauer, T. Kubis, M. Sabathil, A. Trellakis, and P. Vogl, IEEE Trans. Electron Devices **54**, 2137 (2007).
[40] T. P. Pearsall, F. H. Pollak, J. C. Bean, and R. Hull, Phys. Rev. B **33**, 6821 (1986).

[41]M. Cardona and N. E. Christensen, Phys. Rev. B **37**, 1011 (1988).
[42]G. P. Schwartz, M. S. Hybertsen, J. Bevk, R. G. Nuzzo, J. P. Mannaerts, and G. J. Gualtieri, Phys. Rev. B **39**, 1235 (1989).
[43]J. F. Morar, P. E. Batson, and J. Tersoff, Phys. Rev. B **47**, 4107 (1993).
[44]A. Franceschetti, S.-H. Wei, and A. Zunger, Phys. Rev. B **50**, 17797 (1994).
[45]Y.-H. Li, A. Walsh, S. Chen, W.-J. Yin, J.-H. Yang, J. Li, J. L. F. Da Silva, X. G. Gong, and S.-H. Wei, Appl. Phys. Lett. **94**, 212109 (2009).
[46]A. R. Goñi, K. Syassen, and M. Cardona, Phys. Rev. B **39**, 12921 (1989).
[47]Y.-H. Li, X. G. Gong, and S.-H. Wei, Phys. Rev. B **73**, 245206 (2006).
[48]M. V. Fischetti and S. E. Laux, J. Appl. Phys. **80**, 2234 (1996).
[49]G. A. Northrop, J. F. Morar, D. J. Wolford, and J. A. Bradley, Appl. Phys. Lett. **61**, 192 (1992).
[50]F. Cerdeira, C. J. Buchenauer, F. H. Pollak, and M. Cardona, Phys. Rev. B **5**, 580 (1972).
[51]E. Anastassakis, A. Cantarero, and M. Cardona, Phys. Rev. B **41**, 7529 (1990).
[52]D. Olego and M. Cardona, Phys. Rev. B **25**, 1151 (1982).
[53]B. A. Weinstein and G. J. Piermarini, Phys. Rev. B **12**, 1172 (1975).
[54]J. Liu, D. D. Cannon, K. Wada, Y. Ishikawa, D. T. Danielson, S. Jongthammanurak, J. Michel, and L. C. Kimerling, Phys. Rev. B **70**, 155309 (2004).
[55]L. D. Laude, F. H. Pollak, and M. Cardona, Phys. Rev. B **3**, 2623 (1971).
[56]M.-F. Li, X.-S. Zhao, Z.-Q. Gu, J.-X. Chen, Y.-J. Li, and J.-Q. Wang, Phys. Rev. B **43**, 14040 (1991).
[57]D. V. Lang, R. People, J. C. Bean, and A. M. Sergent, Appl. Phys. Lett. **47**, 1333 (1985).
[58]J. Weber and M. I. Alonso, Phys. Rev. B **40**, 5683 (1989).